ACS APPLIED MATERIALS & INTERFACES

Letter

www.acsami.org

In Situ Electrochemical ELISA for Specific Identification of Captured Cancer Cells

Tina Saberi Safaei,[†] Reza M. Mohamadi,[‡] Edward H. Sargent,[†] and Shana O. Kelley*[,‡,§,⊥]

[†]Department of Electrical and Computer Engineering, Faculty of Applied Science and Engineering, University of Toronto, 10 King's College Road, Toronto, Ontario M5S 3G4, Canada

[‡]Department of Pharmaceutical Sciences, Leslie Dan Faculty of Pharmacy, University of Toronto, 144 College Street, Toronto, Ontario M5S 3M2, Canada

[§]Institute for Biomaterials and Biomedical Engineering, University of Toronto, 164 College Street Toronto, Ontario M5S 3G9, Canada

[⊥]Department of Biochemistry, Faculty of Medicine, University of Toronto, 1 King's College Circle, Toronto, Ontario M5S 1A8, Canada

Supporting Information

ABSTRACT: Circulating tumor cells (CTCs) are cancer cells disseminated from a tumor into the bloodstream. Their presence in patient blood samples has been associated with metastatic disease. Here, we report a simple system that enables the isolation and detection of these rare cancer cells. By developing a sensitive electrochemical ELISA method integrated within a microfluidic cell capture system, were we able to reliably detect very low levels of cancer cells in whole blood. Our results indicate that the new system provides the clinically relevant specificity and sensitivity needed for a convenient, point-of-need assay for cancer cell counting.

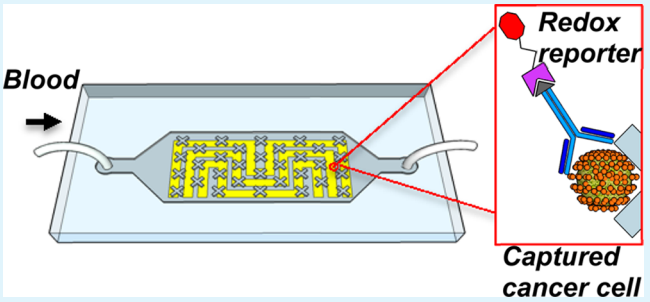

KEYWORDS: *cancer cell detection, electrochemistry, cancer cell isolation, microfluidics, integrated chip*

Circulating tumor cells (CTC) can provide information about the stage of disease, tumor phenotype and effectiveness of therapy.[1−3] Early detection of CTCs in the bloodstream at very low concentrations could provide a pathway to early diagnosis of cancer and, as a result, more effective disease management. However, CTCs are very rare in whole blood, with billions of healthy blood cells present in a sample that may contain only a few CTCs.

The rarity of CTCs in the blood imposes demanding requirements for sensitivity and specificity in CTC isolation and detection. To this end, many systems have been developed that use pre-enrichment of CTCs and/or dilution of blood samples to facilitate isolation and analysis.[4−7] Many CTC detection techniques rely on fluorescence imaging, which relies both on skill on the part of the operator and on costly instrumentation.[4−8] Alternative readout approaches using the quartz crystal microbalance,[9] micro NMR spectroscopy,[10] micro-Hall detectors,[11] surface-enhanced Raman spectroscopy,[12] lateral flow[13] and electrical impedance spectroscopy[14] have each been reported in recent years to offer significant advantages over legacy CTC methods.

Electrochemical sensing techniques have been investigated for CTC detection in light of their simplicity and resultant low cost.[15−26] To date, however, all reported electrochemical techniques fail to meet sensitivity specifications for clinical applications. Whereas detection limits would ideally be below 2 cells mL^{-1}, all prior electrochemical reports exhibit detection limits that exceed 100 cells mL^{-1}. The ability to process multi-mL blood samples in clinically actionable times is a further requirement yet to be fulfilled by previously reported electrochemical CTC technologies. Finally, electrochemical CTC sensors have yet to be validated in the detection of target cells in whole blood.

Here we report a microfabricated system that uses both microscale and nanoscale phenomena to isolate and detect cancer cells on-chip (Figure 1). The integrated circuit comprises patterned microstructures that facilitate cell capture printed on top of a glass substrate containing patterned gold structures that are used for electrochemical readout (Figure 1a). The capture method is based on the previously reported velocity valley (VV) chip.[27] The expression of the epithelial cell adhesion molecule (EpCAM) is commonly used to target and capture cancer cells,[26,28,29] and here, cells are specifically labeled with magnetic nanobeads conjugated with the anti-EpCAM antibody and then introduced into the capture chip sandwiched between two arrays of magnets. The amplitude of the magnetic

Received: March 19, 2015
Accepted: May 4, 2015

DOI: 10.1021/acsami.5b02404
ACS Appl. Mater. Interfaces XXXX, XXX, XXX−XXX

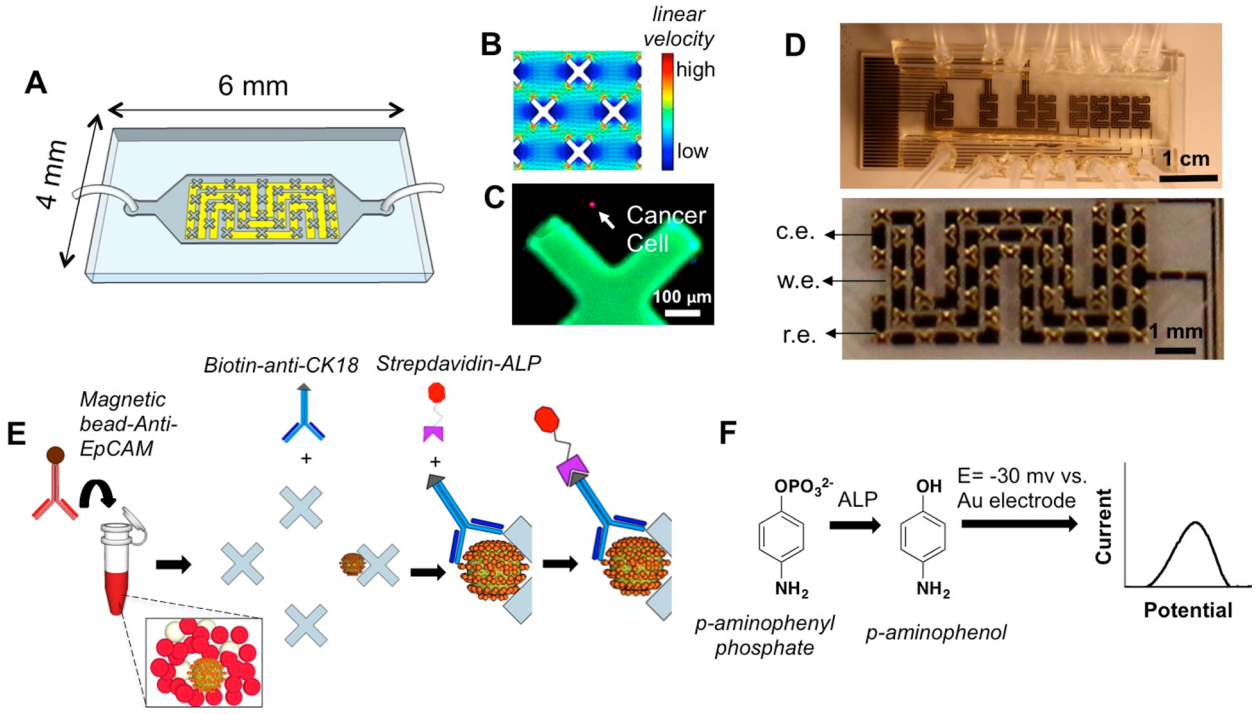

Figure 1. Cancer cell capture and electrochemical detection method. (A) Schematic of chip design, showing the capturing well with X-shaped posts and on-chip electrodes. (B) COMSOL simulation of linear velocity gradient, indicating the velocity valley regions around X-shaped posts. (C) Immunofluorescent image of a captured cancer cell on chip. (D) Image of a chip with 8 independent sensors and a zoomed in view of one sensing chamber, showing on-chip reference, counter, working electrodes and X-shaped posts. Small dimensions of wells allow further multiplexing and parallel detection of cancer cells on one chip. (E) Cancer cells are tagged with magnetic nanoparticles functionalized with anti-EpCAM antibody. These cells get captured in the low flow regions created by velocity valleys. Afterward, they are functionalized on-chip with biotinylated anti-CK18 and streptavidin-alkaline phosphatase conjugates in two subsequent steps. (F) Alkaline phosphatase molecules convert *p*-aminophenyl phosphate to *p*-aminophenol. The electroactive *p*-aminophenol gets oxidized at the potential of −30 mV against Au reference electrode. The generated signal is indicative of presence of a cell and its intensity is proportional to the number of captured cells.

field generated is insufficient—in an open channel - to overcome the drag force of the cells, and the chip fails to capture the magnetic-particle-labeled cancer cells. When X-shaped posts are included within the channel, they decrease the local velocity of the fluid, thereby decreasing the drag force (Figure 1b). As a result, cells having high magnetic particle labeling (corresponding to high surface biomarker expression) are robustly captured (Figure 1c).

The electrochemical measurements were carried out on-chip using a 3-electrode configuration. The active area of the reference, working and counter electrodes are ∼3 mm^2. The on-chip electrodes are arranged as shown in Figure 1d in order to keep the distance between them constant and as small as possible. This design alleviates the possible potential drop resulting from solution resistance throughout the chamber.

The in situ on-chip detection is based on an electrochemical enzyme-linked immunosorbent assay (EC-ELISA). Cancer cell detection is carried out on-chip, in-line with cell capture. Captured cells are tagged with an antibody against a universal epithelial cancer marker (cytokeratin, CK). The anti-CK18 antibody is labeled with alkaline phosphatase (ALP) based on biotin—streptavidin binding (Figure 1e). In this assay, ALP is used to convert *p*-aminophenyl phosphate (p-APP) to an electrochemically active reagent (*p*-aminophenol) through an enzymatic reaction. p-Aminophenol (p-AP) is then oxidized electrochemically and the signal is read as a change in the current (Figure 1f). The intensity of the electrochemical signal therefore depends on the number of cells captured in that chamber, enabling the enumeration of cells. Moreover, the enzyme molecules are not consumed in this reaction, which results in amplified production of p-AP. The catalytic nature of the reaction enables detection of low number of cells and makes our detection method very sensitive. It should be noted that all of the binding steps were performed on-chip and under continuous flow of reagents. However, to prevent the loss of redox species, flow was stopped during p-APP incubation and the electrochemical sampling period. During the incubation time, degree of generation and diffusion of redox species are high enough that electrochemical signals are independent of the position of captured cancer cells relative to the electrodes.

The performance of the in situ ELISA approach was evaluated by monitoring the electrochemical response of various concentrations of the electrochemical reporter group p—aminophenol (p-AP) in TBS buffer. Differential pulse voltammetry reveals an oxidation peak centered at −0.03 V vs on-chip gold electrodes, which corresponds to the oxidation potential of p-AP. The intensity of the signals grows as the concentration of the analyte is increased, and no signal was detected in the absence of electroactive species (DPV of TBS shows no signal in this potential window) (Figure 2). We observed that the lowest reproducibly detectable concentration of p-AP is ∼1 μM. The incubation time for the enzymatic reaction and the concentration of the added enzyme were optimized to stay above this limit for detection of target cells.

We validated the high levels of sensitivity of the chip in detection of rare cancer cells by sensing different concen-

DOI: 10.1021/acsami.5b02404
ACS Appl. Mater. Interfaces XXXX, XXX, XXX−XXX

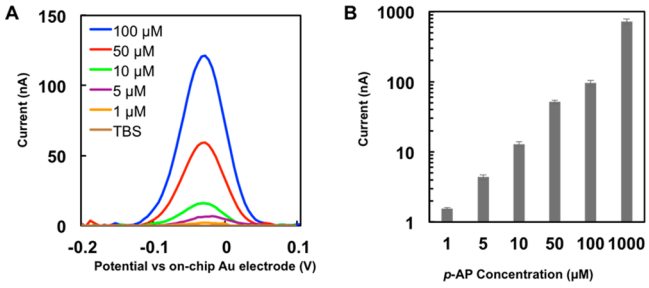

Figure 2. Evaluation of on-chip electrode performance and p-AP oxidation signal. (A) DPV results show the oxidation peak of *p*-AP at the potential of −30 mV against on-chip electrodes. No signal was detected from TBS buffer in this potential window. (B) Quantitation of the oxidation peaks amplitude produced at −30 mV against on-chip electrodes with different concentrations of *p*-AP in aTBS buffer. The measurements were carried out in the potential window of −200 mV to 200 mV with potential step of 5 mV, pulse amplitude of 50 mV, pulse width 50 ms, and a pulse period of 100 ms.

trations of VCaP cells. These cells are an important epithelial cancer cell model and express the surface antigen used for capture, EpCAM. The cells were captured on the VV chip and analyzed using in situ ELISA. The results demonstrate the capability of the chip to detect as few as one captured cancer cell (Figure 3a).

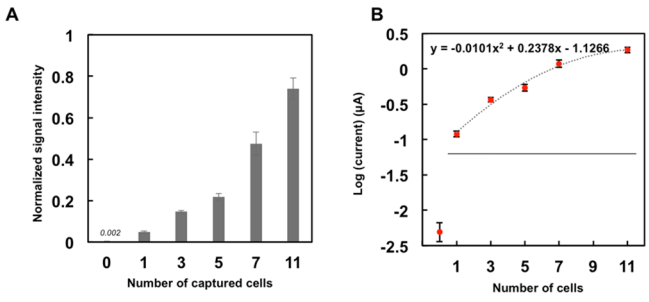

Figure 3. Enumeration of cancer cells. (A) Signals from electrochemical ELISA were collected for detection of VCaP cells. Afterward, the number of captured cells was verified using immunofluorescence technique. (B) Logarithmic relation correlates signal intensity to the number of captured cells.

The actual number of cells captured was independently verified by performing immunostaining and fluorescence microscopy on each chip and correlating the captures cell numbers with obtained electrochemical signals. The logarithmic relation between intensity of collected signals and the number of captured cells enables the quantitative enumeration of rare cells (Figure 3b). The results were highly reproducible, as evidenced by the low error values shown in Figure 3. It should be noted that data normalization was accomplished by dividing the signal intensities by the maximum value of each corresponding graph.

The logarithmic relation observed in Figure 3b is due to the catalytic behavior of the enzyme and the resulting p-AP production amplification, whereas in the case of Figure 2, there is no enzymatic reaction involved and p-AP solutions were ready-made, therefore the signal intensity increases linearly with increasing concentration of the solutions.

We sought next to assess the performance of the chip when it is challenged with an abundance of blood cells. We investigated whether it would have clinically relevant specificity by attempting the capture and detection of VCaP cells spiked in whole blood (Figure 4). To study the capture efficiency of the chip, we tested different concentrations of cancer cells in blood. The number of captured cancer cells was extracted from immunofluorescence images. To distinguish between cancer cells and white blood cells, triple stains targeting cell nuclei, CD45 (a surface marker specific for WBC) and CK18 (a surface marker specific for cancer cells) were used. The obtained capture efficiency for the intended cancer cells was on average 85% (Figure 4a). Along with the capture of cancer cells, on average of about 80 white blood cells were captured nonspecifically in the chips. This level of nonspecific capture is much lower than what has been observed in other cancer cell isolation techniques.

It is noteworthy that higher levels of error were observed when higher numbers of cancer cells were present in samples. This trend relates to the design and mechanism of function of the VV chip. We have previously reported detailed calculations and simulation data for the spatial distribution of linear velocities of cells in the presence of X-shaped capture structures used in the VV chip. At the flow rate employed, only 24% of the chip area has linear velocities lower than the threshold required for effective capture of typical magnetically labeled cells employed in this work (see the Supporting Information).[30] Moreover, we have observed that the capture efficiency decreases as the number of captured cancer cells per well exceeds 20 (equal to 60 cancer cells per ml of blood). It is on this basis that we explain lower reproducibility and larger error bars in the capture of more than 20 cells. This could in future be addressed by increasing the well size to serve applications in which higher captured-cell numbers were of interest.

As shown Figure 4b, detection of as low as two spiked cells in each milliliter of whole blood was achieved. The system therefore remains highly sensitive even in the presence of abundance of nonspecific cells. Nevertheless, the complexity of blood media and the consequent nonspecific bindings resulted in a higher background signal relative to what has been observed when detecting cancer cells in buffer. Signal intensities in general are decreased for blood samples, which is attributed to nonspecific partial coverage of the surface of electrodes by white blood cells (compare Figures 3b and 4c). The signal intensity and the number of cells were correlated using the equation displayed in Figure 4c. This fit will allow us to extract the number of cells present in blood samples from the amplitude of the obtained electrochemical current. As displayed in Figure 4a, the calculated number of cells is in good agreement with the counted number of captured cells in immunofluorescent microscopy images (a representative image of cancer cell is displayed in Figure 4d).

The remarkably high sensitivity of the system especially in comparison to the other electrochemical techniques is due to the enzymatic nature of the assay. Enzyme molecules biospecifically bound to the target cells will amplify the number of electroactive species generated per each cell. As a result, higher signal-to-noise ratio is achieved, which translates to higher sensitivity of the immunosensor.

In summary, we validated a chip-based system that enables capture and enumeration of very low concentrations of cancer cells. This method requires only simple instrumentation and has the potential to become very cost-effective, via automation, compared to conventional immunostaining approaches. Because it can be tailored to employ different capture or labeling antibodies, the system can readily be adapted to

DOI: 10.1021/acsami.5b02404
ACS Appl. Mater. Interfaces XXXX, XXX, XXX−XXX

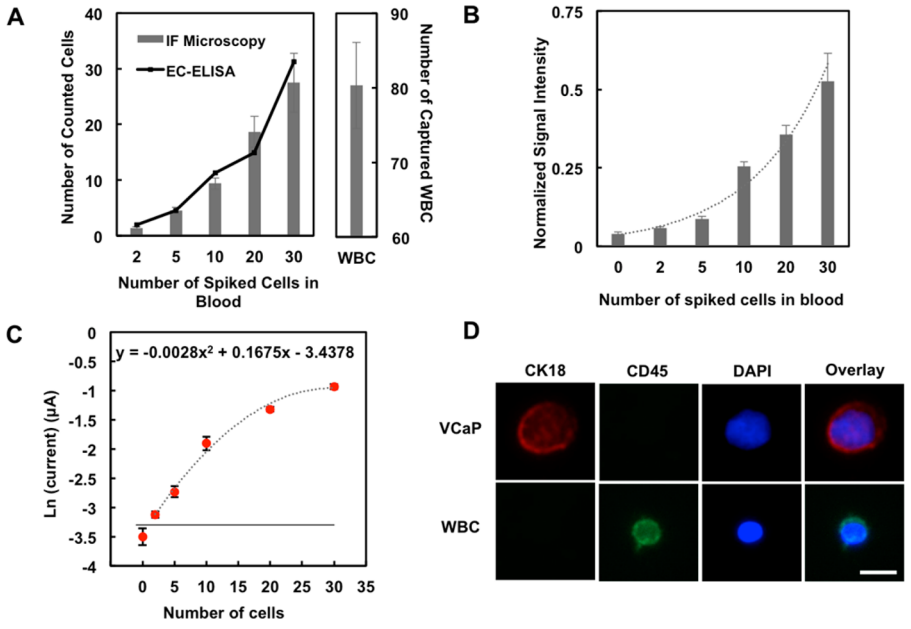

Figure 4. Evaluation of performance with blood samples. (A) Immunofluorescence microscopy was used to investigate the capture efficiency of chip for VCaP cells in whole blood and the nonspecific capture of WBCs. The calculated number of cells from EC-ELISA measurements are also displayed on the graph. (B) Different concentrations of VCaP cells spiked in whole blood were detected using electrochemical ELISA. (C) A logarithmic relation correlates signal intensity to the number of spiked cells. A cutoff threshold of −3.25 was established as the minimum current required for a positive result. (D) Representative immunofluorescence images of a VCaP cell and a WBC. The scale bar is indicative of 10 μm and all the images are to the scale.

different cancer cell types. It offers a significant advantage over commercially available systems which require much higher levels of hands on processing time and subjective data interpretation (Figure S2 in the Supporting Information). The level of sensitivity and the ability to analyze whole blood samples exhibit excellent performance compared to previously reported electrochemical cancer cell capture and sensing solutions.

■ ASSOCIATED CONTENT

Supporting Information

Details about experimental methods, chip surface area percentage for the effective capture of cells, image of nonspecifically captured WBCs, and step-by-step comparison of EC-ELISA VV chip and CellSearch. The Supporting Information is available free of charge on the ACS Publications website at DOI: 10.1021/acsami.5b02404.

■ AUTHOR INFORMATION

Corresponding Author

*E-mail: shana.kelley@utoronto.ca.

Author Contributions

The manuscript was written through contributions of all authors. All authors have given approval to the final version of the manuscript.

Notes

The authors declare no competing financial interest.

■ ACKNOWLEDGMENTS

The authors wish to thank the Canadian Institutes for Health Research for an Emerging Team Grant, the Ontario Ministry of Research and Innovation for support from the Ontario Research Fund, the Canadian Cancer Research Society for an Innovation Grant, and the Connaught Fund.

■ REFERENCES

(1) Hou, J.; Krebs, M.; Ward, T.; Sloane, R.; Priest, L.; Hughes, A.; Clack, G.; Ranson, M.; Blackhall, F.; Dive, C. Circulating Tumor Cells as a Window on Metastasis Biology in Lung Cancer. *Am. J. Pathol.* **2011**, *178*, 989−996.

(2) Craig Miller, M.; Doyle, G. V.; Terstappen, L. W. M. M. Significance of Circulating Tumor Cells Detected by the CellSearch System in Patients with Metastatic Breast Colorectal and Prostate Cancer. *J. Oncol.* **2009**, 2010, Article ID 617421.

(3) Rack, B.; Schindlbeck, C.; Jückstock, J.; Andergassen, U.; Hepp, P.; Zwingers, T.; Friedl, W. P. T.; Lorenz, R.; Tesch, H.; Fasching, P. A.; Fehm, T.; Schneeweiss, A.; Lichtenegger, W.; Beckmann, M. W.; Friese, K.; Pantel, K.; JannI, W. J. Circulating Tumor Cells Predict Survival in Early Average-to-high Risk Breast Cancer Patients. *J. Natl. Cancer Inst.* **2014**, *106*, dju066.

(4) Paterlini-Brechot, P.; Benali, N. L. Circulating Tumor Cells (CTC) Detection: Clinical Impact and Future Directions. *Cancer Lett.* **2007**, *253*, 180−204.

(5) Pantel, K.; Alix-Panabières, C. Circulating Tumour Cells in Cancer Patients: Challenges and Perspectives. *Trends Mol. Med.* **2010**, *16*, 398−406.

(6) Farace, F.; Massard, C.; Vimond, N.; Drusch, F.; Jacques, N.; Billiot, F.; Laplanche, A.; Chauchereau, A.; Lacroix, L.; Planchard, D.; Le Moulec, S.; André, F.; Fizazi, K.; Soria, J. C.; Vielh, P. A Direct Comparison of CellSearch and ISET for Circulating Tumour-cell Detection in Patients with Metastatic Carcinomas. *Br. J. Cancer* **2011**, *105* (6), 847−853.

(7) Andreopoulou, E.; Yang, L.-Y.; Rangel, K. M.; Reuben, J. M.; Hsu, L.; Krishnamurthy, S.; Valero, V.; Fritsche, H. A.; Cristofanilli, M. Comparison of Assay Methods for Detection of Circulating Tumor Cells in Metastatic Breast Cancer: AdnaGen AdnaTest BreastCancer Select/Detect versus Veridex CellSearch System. *Int. J. Cancer* **2012**, *130*, 1590−1597.

(8) Nagrath, S.; Sequist, L. V.; Maheswaran, S.; Bell, D. W.; Irimia, D.; Ulkus, L.; Smith, M. R.; Kwak, E. L.; Digumarthy, S.; Muzikansky, A.; Ryan, P.; Balis, U. J.; Tompkins, R. G.; Haber, D. A.; Toner, M. Isolation of Rare Circulating Tumour Cells in Cancer Patients by Microchip Technology. *Nature* **2007**, *450*, 1235−1239.

DOI: 10.1021/acsami.5b02404
ACS Appl. Mater. Interfaces XXXX, XXX, XXX−XXX

(9) Pan, Y.; Guo, M.; Nie, Z.; Huang, Y.; Pan, C.; Zeng, K.; Zhang, Y.; Yao, S. Selective Collection and Detection of Leukemia Cells on a Magnet-quartz Crystal Microbalance System Using Aptamer-conjugated Magnetic Beads. *Biosens. Bioelectron.* **2010**, *225*, 1609−1614.
(10) Ghazani, A. A.; Castro, C. M.; Gorbatov, R.; Lee, H.; Weissleder, R. Sensitive and Direct Detection of Circulating Tumor Cells by Multimarker μ-Nuclear Magnetic Resonance. *Neoplasia* **2012**, *14*, 388−395.
(11) Issadore, D.; Chung, J.; Shao, H.; Liong, M.; Ghazani, A. A.; Castro, C. M.; Weissleder, R.; Lee, H. Ultrasensitive Clinical Enumeration of Rare Cells ex-Vivo Using a Micro-hall Detector. *Sci. Transl. Med.* **2012**, *4*, 141ra92−141ra92.
(12) Sha, M. Y.; Xu, H.; Natan, M. J.; Cromer, R. Surface-enhanced Raman Scattering Tags for Rapid and Homogeneous Detection of Circulating Tumor Cells in the Presence of Human Whole Blood. *J. Am. Chem. Soc.* **2008**, *9130*, 17214−17215.
(13) Liu, G.; Mao, X.; Phillips, J. A.; Xu, H.; Tan, W.; Zeng, L. Aptamer−nanoparticle Strip Biosensor for Sensitive Detection of Cancer Cells. *Anal. Chem.* **2009**, *81*, 10013−10018.
(14) Chung, Y.; Reboud, J.; Chuan Lee, K.; Min Lim, H.; Yi Lim, P.; Yanping Wang, K.; Cheong Tang, K.; Ji, H.; Chen, Y. An Electrical Biosensor for the Detection of Circulating Tumor Cells. *Biosens. Bioelectron.* **2011**, *26*, 2520−2526.
(15) Feng, L.; Chen, Y.; Ren, J.; Qu, X. A Graphene Functionalized Electrochemical Aptasensor for Selective Label-free Detection of Cancer Cells. *Biomaterials* **2011**, *32*, 2930−2937.
(16) Cheng, W.; Ding, L.; Ding, S.; Yin, Y.; Ju, H. A Simple Electrochemical Cytosensor Array for Dynamic Analysis of Carcinoma Cell Surface Glycans. *Angew. Chem.* **2009**, *121*, 6587−6590.
(17) Li, J.; Xu, M.; Huang, H.; Zhou, J.; Abdel-Halimb, E. S.; Zhang, J.; Zhu, J. Aptamer-quantum Dots Conjugates-based Ultrasensitive Competitive Electrochemical Cytosensor for the Detection of Tumor Cell. *Talanta* **2011**, *85*, 2113−2120.
(18) Maltez-da Costa, M.; de la Escosura-Muñiz, A.; Nogués, C.; Barrios, L.; Ibáñez, E.; Merkoçi, A. Detection of Circulating Cancer Cells Using Electrocatalytic Gold Nanoparticles. *Small* **2012**, *8*, 3605−3612.
(19) Moscovici, M.; Bhimji, A.; Kelley, S. O. Rapid and Specific Electrochemical Detection of Prostate Cancer Cells Using an Aperture Sensor Array. *Lab Chip* **2013**, *13*, 940−946.
(20) Zhu, Y.; Chandra, P.; Shim, Y. Ultrasensitive and Selective Electrochemical Diagnosis of Breast Cancer Based on a Hydrazine−Au Nanoparticle−aptamer Bioconjugate. *Anal. Chem.* **2012**, *85*, 1058−1064.
(21) Wu, Y.; Xue, P.; Hui, K. M.; Kang, Y. Electrochemical-and Fluorescent-Mediated Signal Amplifications for Rapid Detection of Low-Abundance Circulating Tumor Cells on a Paper-Based Microfluidic Immunodevice. *ChemElectroChem.* **2014**, *1*, 722−727.
(22) Wan, Y.; Zhou, Y.; Poudineh, M.; Saberi Safaei, T.; Mohamadi, R. M.; Sargent, E. H.; Kelley, S. O. Highly Specific Electrochemical Analysis of Cancer Cells Using Multi-Nanoparticle Labeling. *Angew. Chem., Int. Ed.* **2014**, *53*, 13145−13149.
(23) Chen, X.; Wang, Y.; Zhang, Y.; Chen, Z.; Liu, Y.; Li, Z.; Li, J. Sensitive Electrochemical Aptamer Biosensor for Dynamic Cell Surface N-Glycan Evaluation Featuring Multivalent Recognition and Signal Amplification on a Dendrimer−Graphene Electrode Interface. *Anal. Chem.* **2014**, *86*, 4278−4286.
(24) Kimmel, D. W.; LeBlanc, G.; Meschievitz, M. E.; Cliffel, D. E. Electrochemical Sensors and Biosensors. *Anal. Chem.* **2011**, *84*, 685−707.
(25) Ivanov, I.; Stojcic, J.; Stanimirovic, A.; Sargent, E. H.; Kelley, S. O. Chip-Based Nanostructured Sensors Enable Accurate Identification and Classification of Circulating Tumor Cells in Prostate Cancer Patient Blood Samples. *Anal. Chem.* **2013**, *85*, 398−403.
(26) Zhang, P.; Chen, L.; Xu, T.; Liu, H.; Liu, X.; Meng, J.; Yang, G.; Jiang, L.; Wang, S. Programmable Fractal Nanostructured Interfaces for Specific Recognition and Electrochemical Release of Cancer Cells. *Adv. Mater.* **2013**, *25*, 3566−3570.
(27) Mohamadi, R. M.; Besant, J. D.; Mepham, A.; Green, B.; Mahmoudian, L.; Gibbs, T.; Ivanov, I.; Malvea, A.; Stojcic, J.; Allan, A. L.; Lowes, L. E.; Sargent, E. H.; Nam, R. K.; Kelley, S. O. Nanoparticle-Mediated Binning and Profiling of Heterogeneous Circulating Tumor Cell Subpopulations. *Angew. Chem., Int. Ed.* **2014**, *54*, 139−143.
(28) Liu, H.; Liu, X.; Meng, J.; Zhang, P.; Yang, G.; Su, B.; Sun, K.; Chen, L.; Han, D.; Wang, S.; Jiang, L. Hydrophobic Interaction-Mediated Capture and Release of Cancer Cells on Thermoresponsive Nanostructured Surfaces. *Adv. Mater.* **2013**, *25*, 922−927.
(29) Yang, G.; Liu, H.; Liu, X.; Zhang, P.; Huang, C.; Xu, T.; Jiang, L.; Wang, S. Underwater-Transparent Nanodendritic Coatings for Directly Monitoring Cancer Cells. *Adv. Healthcare Mater.* **2014**, *3*, 332−337.
(30) Besant, J. D.; Mohamadi, R. M.; Aldridge, P. M.; Li, Y.; Sargent, E. H.; Kelley, S. O. Velocity Valleys Enable Efficient Capture and Spatial Sorting of Nanoparticle-bound Cancer Cells. *Nanoscale* **2015**, *7*, 6278−6285.

DOI: 10.1021/acsami.5b02404
ACS Appl. Mater. Interfaces XXXX, XXX, XXX−XXX